

## Article

# Conversion of Waste Corn Straw to Value-Added Fuel via Hydrothermal Carbonization after Acid Washing

Shulun Han <sup>1</sup> , Li Bai <sup>2,\*</sup> , Mingshu Chi <sup>1</sup>, Xiuling Xu <sup>3</sup>, Zhao Chen <sup>1</sup> and Kecheng Yu <sup>1</sup>

<sup>1</sup> School of Municipal and Environmental Engineering, Jilin Jianzhu University, Changchun 130118, China; hsl34hsl@126.com (S.H.); cms20062006@163.com (M.C.); chenzhao0703@163.com (Z.C.); yukecheng00@163.com (K.Y.)

<sup>2</sup> Key Laboratory of Songliao Aquatic Environment Ministry of Education, Jilin Jianzhu University, Changchun 130118, China

<sup>3</sup> Library of Jilin Jianzhu University, Jilin Jianzhu University, Changchun 130118, China; xuxiuling@iccas.ac.cn

\* Correspondence: baili@jlju.edu.cn

**Abstract:** To enhance the hydrothermal carbonization (HTC) process on biomass waste and improve the quality of biomass solid fuel. Corn straw was pretreated with acid washing and subsequently hydrothermally carbonized at 180–270 °C. The solid product obtained (hydrochars) was compared with the solid product produced from untreated hydrothermally carbonized straw. The results show that the acid pretreatment removed 7.9% of the ash from the straw. ICP and XRD analysis show that most of the alkali and alkaline earth metals have been removed. This addresses the defect of high ash content as the HTC temperature increases. The HHV of hydrochars produced by HTC after acid washing can reach 27.7 MJ/kg, which is nearly 10% higher than that of hydrochars prepared without acid washing pretreatment, and nearly 70% higher than that of straw raw materials. Elemental analysis and FTIR analysis show that the acid washing pretreatment changed the content and structure of the biomass components in the straw, resulting in a more complete HTC reaction and higher carbon sequestration. The decrease of H/C and O/C deepened the degree of coal-like transformation of hydrochars, with the lowest approaching the bituminous coal zone. The combustion characteristics of the hydrochars prepared after acid washing were significantly upgraded, the comprehensive combustion index and thermal stability of hydrochars both increased. Therefore, HTC after acid washing pretreatment is beneficial to further improve the high heating value and combustion characteristics of hydrochar.

**Keywords:** waste straw; biomass fuel; hydrothermal carbonization; acid washing; high heating value



**Citation:** Han, S.; Bai, L.; Chi, M.; Xu, X.; Chen, Z.; Yu, K. Conversion of Waste Corn Straw to Value-Added Fuel via Hydrothermal Carbonization after Acid Washing. *Energies* **2022**, *15*, 1828. <https://doi.org/10.3390/en15051828>

Academic Editors: Abdul-Ghani Olabi, Michele Dassisti and Zhien Zhang

Received: 9 January 2022

Accepted: 24 February 2022

Published: 2 March 2022

**Publisher's Note:** MDPI stays neutral with regard to jurisdictional claims in published maps and institutional affiliations.



**Copyright:** © 2022 by the authors. Licensee MDPI, Basel, Switzerland. This article is an open access article distributed under the terms and conditions of the Creative Commons Attribution (CC BY) license (<https://creativecommons.org/licenses/by/4.0/>).

## 1. Introduction

As a major agricultural country, China has produced more than 900 million tons of waste straw every year. As a source of biomass energy, straw has become the world's fourth-largest energy source after coal, oil, and natural gas [1]. The rational use of straw can not only solve the waste of straw and protect the environment, but more importantly, it can replace traditional fuels and reduce CO<sub>2</sub> emissions while alleviating the increasingly tight fossil fuel reserves [2,3]. Corn straw (CS) has great potential as a solid fuel. However, the high moisture content of straw (about 26%), high transport and storage costs (about \$47.3/tonne), low energy density, high alkali and alkaline earth metal content, and environmental pollution caused by direct combustion limit the use of straw as a solid fuel [4].

Hydrothermal carbonization (also known as wet roasting, HTC) is one of the thermochemical conversion methods [5]. Research on the use of HTC to convert waste biomass into solid fuels, land sorbents, and other applications has received much attention in recent years [6,7]. The process of HTC involves placing biomass and deionized water in a closed vessel and heating it for a period of time under sub-critical water pressure

to a temperature of 180–300 °C. HTC has a unique advantage over treatments such as pyrolysis as it can be carried out without drying the feedstock, thus saving energy, producing a more cohesive carbon structure and being less harmful to the environment [8,9]. Water plays a vital role in the subcritical state, converting from a polar to a non-polar solvent. Water acts as a catalyst in the heating reaction. During HTC, the presence of water reduces the level of activation energy required for bond breakage and therefore allows hydrolysis under relatively mild conditions [10]. Hydrothermal carbonization could effectively improve the combustion characteristics of lignocellulosic biomass [11,12], in Zhang's study [13], the combined combustion index  $S$  of hydrochar prepared from water hyacinth reached  $25.81 (10^{-7} \times \text{min}^{-2} \times \text{°C}^{-3})$  and the thermal stability index  $R_w$  reached  $-28.43 (10^{-5} \times \text{min}^{-1} \times \text{°C}^{-2})$ . The solid product (hydrochars) has a higher high heating value (HHV) than the raw material [14,15]. In the study by Cai [16], tobacco straw reached the HHV of 27.2 MJ/kg for hydrochars at a reaction temperature of 260 °C, which is comparable to burning coal. The HHV also varies depending on the experimental conditions (temperature, pressure, and feedwater pH) [17–19]. The reaction temperature was the most critical factor affecting the HTC [13], with the increased temperature providing energy for the hydrothermal reaction. When the reaction temperature is 160–180 °C, the hemicellulose components in the biomass are hydrolyzed, and xylan will be hydrolyzed into monosaccharides, and further hydrolyzed into small molecular compounds (furfural, etc.) [6]. Cellulose is hydrolysed at 210–230 °C. The long-chain cellulose degrades into oligomers, which then break down into glucose, sugar and 5-methylfurfural [20]. The rest remaining cellulose aggregates together [21]. The chemical structure of lignin is more complex than that of cellulose and hemicellulose. Lignin is a polymer compound consisting of phenylpropane and its derivatives as structural units, which are also bound in more complex ways. It is divided into soluble lignin and insoluble lignin. The water-soluble fraction starts to react at 200 °C, but its content is relatively small and most of the lignin is insoluble [10]. The soluble lignin will be hydrolyzed to form phenolic compounds and the insoluble lignin will remain in the reaction as a solid, similar to the solid-solid form of the reaction in the pyrolysis process [22]. Under low-temperature conditions, the small molecules produced by hydrolysis are polymerized into phenolic coke and eventually undergo aromatization [6]. In addition to these three components, the straw also contains significant amounts of alkali and alkaline earth metals (AAEM), which are the main components of the ash in the hydrochars. The ash content increases with increasing hydrothermal temperature [23]. For biomass fuel, ash content can have a negative impact on biomass HHV [24], ash content also leads to heat transfer barriers in boilers, flue gas pollution, and low combustion efficiency as a fuel [25]. The ash content can also affect the thermochemical conversion of biomass. Therefore, there is a need to find a pretreatment method to reduce the AAEM in the straw and change the composition in the straw, thus further improving the effect of hydrothermal carbonization on the straw. However, there are fewer studies on HTC after pretreatment.

A literature study found that acid washing was the best pretreatment method for the removal of AAEM [26]. In particular, sulfuric acid can not only remove a large amount of AAEM but also change the composition of lignocellulosic biomass [27]. Acid washing breaks some of the hydrogen bonds in hemicellulose, leading to hemicellulose degradation. Sulphuric acid washing also causes the aryl-*o*-ether bond (B-O-4) in lignin to split, destroying the structural properties of the lignin, but the polymerization of the guaiacol group leads to an increase in molecular weight [28]. The effect is more obvious when the concentration is selected as 3% [29].

The main objective of this paper is to reduce the AAEM content in the straw by acid washing pretreatment and to change the internal composition of the straw (cellulose, hemicellulose, lignin, ash content), followed by hydrothermal carbonation experiments at different final temperatures. Fuel properties (calorific value, proximate analysis, degree of coalification), structural characteristics (microcrystalline structure and surface functional group structure), and combustion characteristics of the pretreated hydrothermal carbon were compared and analyzed. The optimization effect of acid pretreatment on hydrother-

mal carbonization was explored, providing a new method for the late thermochemical conversion of waste straw into high-quality solid fuels.

## 2. Materials and Methods

### 2.1. Materials

The waste CS was from the maize-producing areas of Northeast China. The raw material was first rinsed with deionized water, then dried in a blast dryer at 105 °C for 24 h and ground to 50–80 µm (0.27 mm–0.41 mm) using a grinder and a spherical mill.

### 2.2. Acid Washing of Raw Materials

The acid washing was carried out in conical flasks placed in a thermostatic water bath with an acid concentration of 3%, a thermostatic water bath temperature of 4 °C, and a duration of 4 h. The straw after acid washing was rinsed repeatedly with deionized water to neutralize and dried at 85 °C for 24 h. The acid-washed straw is indicated by SCS.

### 2.3. Hydrothermal Carbonization

The dried CS and SCS were weighed 8 g each and prepared with 64 mL of deionized water at a liquid to solid ratio of 1:8 (g/8 mL) into a 100 mL self-stirring low-pressure hydrothermal reactor (K-PSA-100ML, Nanjing ZhengxinInstrument Co., Ltd., Nanjing, China) and purged with inert gas (N<sub>2</sub>) for 5 min. The reaction temperature was set at 180, 210, 240 and 270 °C with a holding time of 60 min at the stirrer speed (120 rpm) and temperature rise rate (20 °C/min) were kept constant under autogenous pressure. After the reaction was complete, the reactor was quickly placed in a constant temperature water bath for cooling. After cooling to room temperature, the gas was removed from the kettle by opening the gas relief valve and the reaction products were separated from the solids by vacuum filtration.

### 2.4. Sample Characterization

#### 2.4.1. Basic Properties

To compare and analyze the basic characteristics of the hydrochars of CS and SCS at different temperatures. Elemental analysis, proximate analysis, and HHV analysis were carried out using an elemental analyzer (EA, Euro Vector EA 3000, Italy), proximate analyzer (YX-GYFX 7705, Changsha Youxin Instrument Manufacturing Co., Ltd., Changsha, China), and an automated calorimeter (YX-ZR/Q 9704, Changsha Youxin Instrument Manufacturing Co., Ltd., ChangSha, China), respectively. The following equations were used to calculate the yield, energy density and energetic recovery efficiency of the products.

$$\text{Hydrochar yield} = (\text{Mass of hydrochar} / \text{Mass of CS}) \times 100\% \quad (1)$$

$$\text{Energy densification} = \text{HHV of hydrochar} / \text{HHV of CS} \quad (2)$$

$$\text{Energetic recovery efficiency} = \text{Hydrochar yield} \times \text{Energy densification} \times 100\% \quad (3)$$

#### 2.4.2. Functional Groups

The microcrystal structure was analyzed using x-ray diffraction (XRDD8prore, Bruker, Germany). XRD spectra were obtained using k-radiation (=0.1542 nm) produced by a voltage of 40 kV and a current of 40 mA. Intensities ranged from 5° to 50° with a continuous scanning rate of 1.8°/min. The surface functional groups of raw materials and hydrochars were characterized by FTIR, and 10 mg of the samples were ground and pressed into sections with 200 mg of KBr for each test. These slices were then measured directly with a Bruker Vertex 70 spectrophotometer over a range of 400–4000 cm<sup>-1</sup> with a cumulative total of 64 scans and a resolution of 4 cm<sup>-1</sup>. The apparent structure of the sample was obtained by electron microscopy (SEM, FEI ESEM QuantaTM 450 FEG, Hillsboro, OR, USA) to monitor the analysis.

### 2.5. Content and Fate of Metals

Metal elements in the samples were detected in an Inductively Coupled Plasma–Optical Emission Spectrometry (ICP-OES, Agilent Technologies Co., Ltd., Santa Clara, CA, USA) after microwave digestion. The supernatant was detected because there still existed precipitation.

The following equations were used to calculate the fate of metal elements [30]:

$$\text{The enrichment rate/removal rate} = (C_{SCS}/C_{cs} - 1) \times 100\% \quad (4)$$

where  $C_{SCS}(\%)$  and  $C_{cs}(\%)$  were the contents of SCS and the raw samples, respectively. Enrichment and removal occur when the content of  $C_{SCS}$  exceeds or is less than that of  $C_{cs}$ .

### 2.6. Determination of Lignocellulose Composition

Cellulose, hemicellulose, and lignin dominate the composition of straw. According to Sluiteretal's research [31], this article uses the NREL/TP-510-42618 method to determine the content of cellulose, hemicellulose, and lignin.

### 2.7. Combustion Characteristics

The combustion of the samples was characterized by using the thermogravimetric analyzer (PE, STA6000). In each test, the initial weight of the sample was maintained at  $10 \pm 0.5$  mg. Throughout the combustion process, the sample was first purged with nitrogen and then the air was continuously supplied at a fixed rate of 100 mL/min. Under the air atmosphere, the experimental temperature was heated from 50 °C to 800 °C at a rate of 20 °C/min. The ignition temperature ( $T_i$ ) and combustion temperature ( $T_f$ ) of the samples could be determined by the method in Ref [32].

To better evaluate the combustion properties, the flammability index  $S$  was calculated and its equation was defined as [13]:

$$S = (dw/dt)_{\max} \times (dw/dt)_{\text{mean}} / (T_i^2 \times T_f) \quad (5)$$

where  $(dw/dt)_{\max}(\%/min)$  and  $(dw/dt)_{\text{mean}}(\%/min)$  referred to the maximum weight loss rate and average weight loss rate, respectively.

The combustion stability index  $R_w$  could evaluate the burning stability of the sample, whose equation was shown as follow:

$$R_w = (dw/dt)_{\max} / (T_i \times T_f) \quad (6)$$

In general, the higher the  $S$  and  $R_w$  indices, the better the combustion characteristics of the sample.

## 3. Results and Discussions

### 3.1. Effect of Acid Washing Pretreatment

It can be seen from Figure 1, the content of inorganic elements in SCS and CS and the removal rate of metals after acid washing. Alkali metals and alkaline earth metal elements are the main elements. These metal elements can coke and slag during combustion, which will cause equipment damage. After acid washing, it can be seen that inorganic elements have been reduced to varying degrees. K and Na are water-soluble ions. In CS, they are generally present as chloride ( $Cl^-$ ), nitrate ( $NO_3^-$ ), and carbonate ( $CO_3^{2-}$ ), and the removal rates after acid washing are 93% and 79.6%, respectively. Ca and Mg ions are water-insoluble/acid-soluble ions. They were adsorbed by carbonate ( $CO_3^{2-}$ ), phosphate ( $PO_4^{3-}$ ), and carboxyl ions (organic part) in the CS [33]. The removal efficiency of these two metal ions by acid washing pretreatment was 96% and 81.2%, respectively. In addition, a small fraction of Si and Fe ions were removed, reaching 21.6% and 8.3%, respectively. The removal method for Si may be mechanical removal during acid washing rather than dissolution. It can be concluded that acid washing will effectively remove AAEM in the CS.

The  $H^+$  in the acid washing would replace the ion exchange process of these AAEM species to achieve the removal effect. In previous studies, when AAEM (especially Ca and Mg) is removed, it will destroy its cross-linking with lignocellulose components [34]. Acid-soluble metal ions have a closer influence on the organic matter in biomass, and they affect the subsequent thermochemical transformation [35]. So the removal of AAEM is beneficial to hydrothermal carbonization.

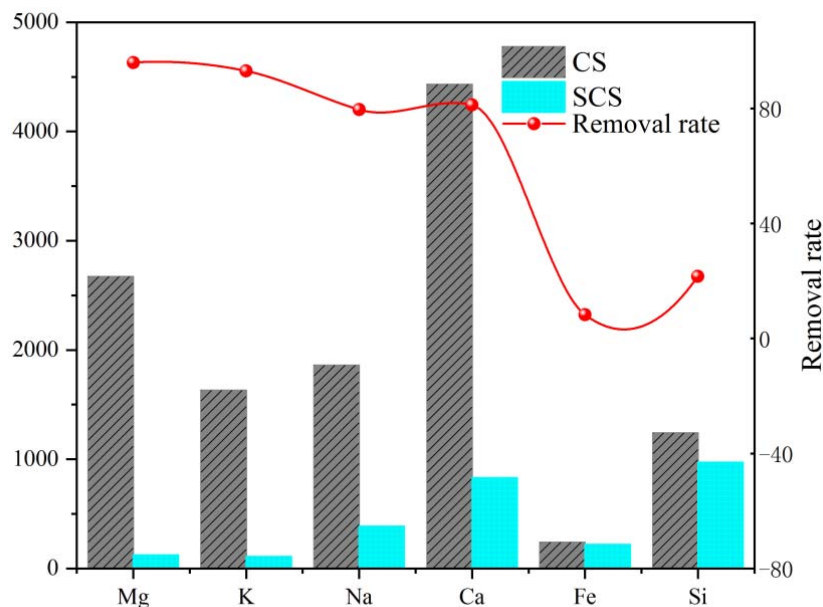


**Figure 1.** The fate of the metal elements CS, SCS.

As can be seen from Table 1, the composition of the CS changed after acid washing. The composition of hemicellulose decreased from 17.8% to 13%, this is because hemicellulose dissolves into monosaccharides such as pentose and hexose after acid washing. The relative content of lignin and cellulose increased. The cellulose content increased from 38.1% to 42.7% and the lignin content increased from 22.5% to 24.3%. Acid washing destroyed the structural properties of the lignin, but polymerization of lignin fragments occurred simultaneously (mainly in the guaiac-based units) and the content of phenolic compounds increased [28]. The increase in the relative content of cellulose and lignin can also be attributed to the reduction of extract content caused by the removal of AAEM after acid washing.

**Table 1.** The relative content of straw components.

Sample	Lignocellulosic Components (%)		
	Hemicellulose	Cellulose	Lignin
CS	17.8 ± 0.05	38.1 ± 0.2	22.5 ± 0.3
SCS	13 ± 0.2	42.7 ± 0.2	24.3 ± 0.2

From the SEM analysis (Figure 2), it can be seen that the SCS surface has a cleaner and more ordered relaxed porous structure compared to the CS. This also validates the idea that the removal of AAEM results in a more relaxed interior of CS, which facilitates thermochemical transformation [36].

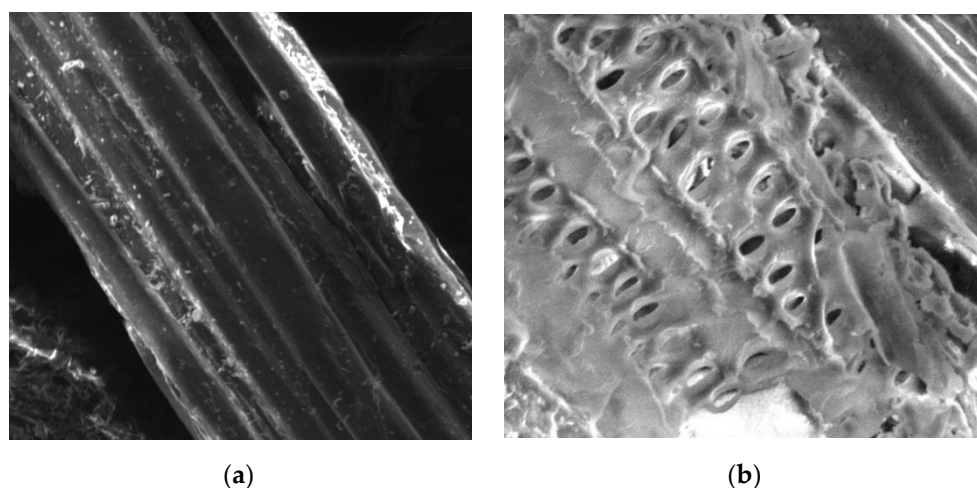


**Figure 2.** Surface morphology of CS, SCS. (a) CS. (b) SCS.

### 3.2. Characteristics of Hydrochar

#### 3.2.1. Solid Yield of Hydrochars

Acid washing had little effect on solid yield, the solid yield of SCS was 92.4% (as shown in Table S1). Figure 3a shows that the yield of hydrochars solids from the HTC process decreases with increasing temperature at different temperatures. The inverse relationship between solid yield and temperature may be due to the more intense thermal decomposition through hydrolysis, dehydration, and decarboxylation at high temperatures [6,37]. At 180 °C and 210 °C, the solid yield of SCS is about 3% lower than that of CS, which can be understood as the relaxation phenomenon inside the straw after acid washing makes the HTC reaction more complete. SCS-HTC-240 and SCS-HTC-270 have a higher solid yield than CS-HTC-240 and CS-HTC-270 because the lower hemicellulose content also means less inhibition of the cellulose small molecule condensation reaction and a more complete liquid-solid phase polymerization reaction [38]. It can be seen from the solid yield that acid washing pretreatment has a positive effect on HTC reaction.

#### 3.2.2. Fuel Properties of Hydrochars

Figure 3b and Table S1 show the proximate analysis of the CS, SCS, and their hydrochars. After acid washing, the ash content of the SCS was significantly reduced, from 14.55% to 6.69%. This is the result of acid washing to remove AAEM. It is supported by 3.1 metal analysis. The ash content of CS increases gradually with increasing temperature. Some of the water-insoluble AAEM reacts with heavy metals and SiO<sub>2</sub> to form silicates, resulting in ash. The ash content of CS-HTC-270 is 21.53%. On the contrary, the acid-soluble AAEM decreased to varying degrees after the acid washing pretreatment, and the increase in ash content of SCS hydrochar was not as large as that of CS hydrochars. At 270 °C, the ash content of SCS is only 10.26%. Ash removal was therefore a necessary step in the conversion of biowaste into alternative renewable fuels. The reduction in ash also represented an increase in the content of combustible components within the CS, and the volatile and fixed carbon content of the SCS increased (67.6% to 72.5% and 17.8% to 20.8%). The volatile content of the SCS-HTC-210 increased by nearly 14% compared to that of the CS-HTC-210. This may be due to the enhanced hydrolysis of cellulose. During the HTC process, the volatile fraction serves two purposes, some is converted to the gas phase and the rest is dissolved into the aqueous phase to produce additional fixed carbon through a repolymerisation reaction [30]. Therefore, it can be seen that at 270 °C, the fixed carbon content of SCS-HTC-270 is higher than that of CS-HTC-270 (40.94~49.07%).

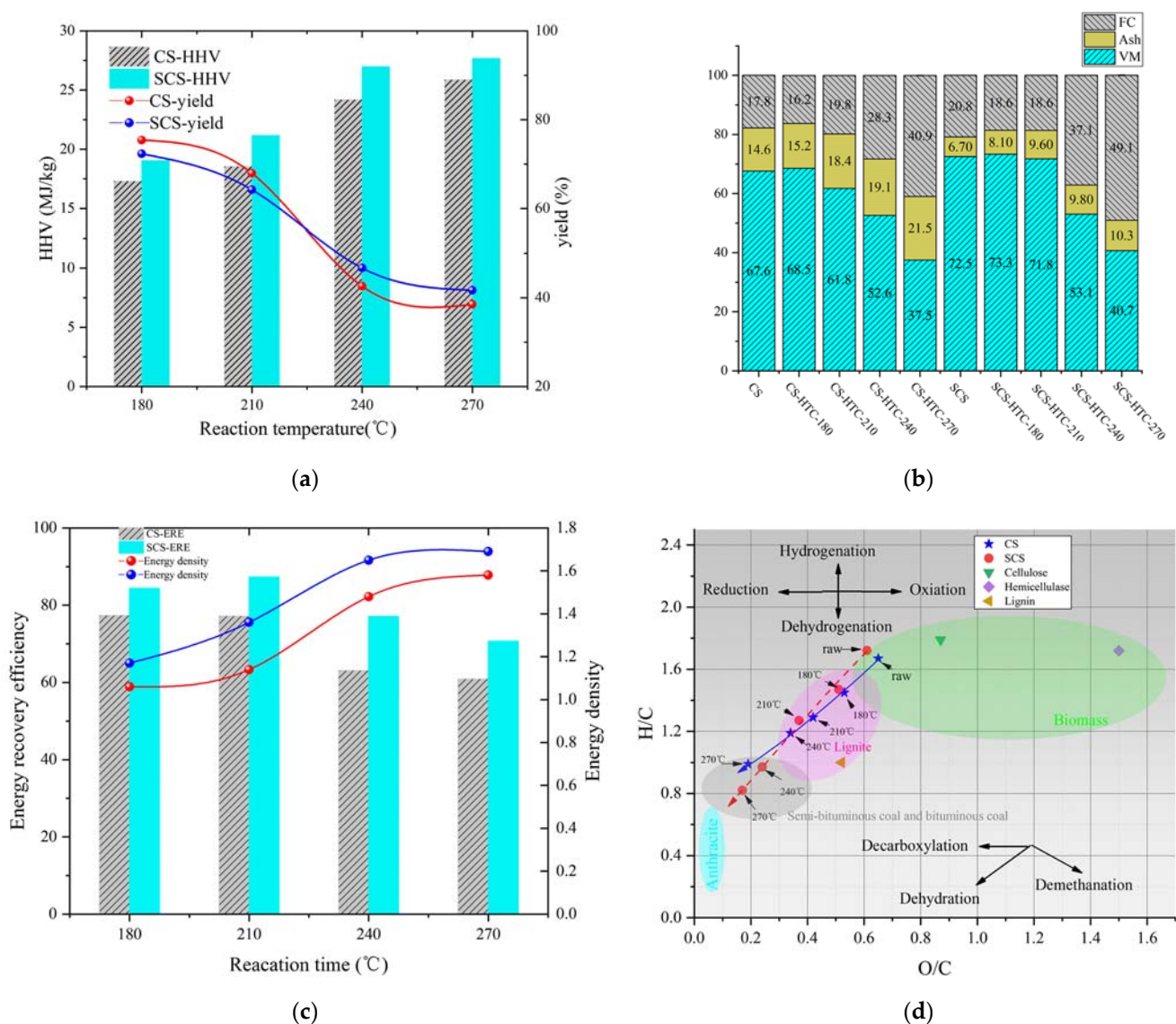


**Figure 3.** Fuel properties of CS, SCS, and their hydrochar. By difference: Fixed carbon% = 100% – volatile matter% – ash% (a) HHV and solid yield (b) Energy density and energy recovery efficiency (c) Proximate analysis (d) Van Krevelen.

As can be seen from Table 1. Acid washing increased the C (41.9~47%) and H (5.8~6.6%) contents in SCS. As the temperature of HTC increased, the C content in CS (41.9~58%) and SCS (47~67%) gradually increased, while the H and O content gradually decreased. Whereas the removal of H and O was the result of increased dehydration and decarboxylation of cellulose and hemicellulose [8]. Hydrogenation and oxidation components in the biomass were decomposed and cracked to form  $H_2$ ,  $CH_4$ ,  $CO_2$ ,  $H_2O$ , and other gases [30]. However, as HTC increases, the C content of SCS increases more than that of CS, and the carbon fixation rate of SCS is higher, especially at 210–240 °C. The growth rate of C content is 3.7% for CS and 8.1% for SCS. The high carbon content represents low H/C and O/C atomic ratios. The variation of the hydrogen to carbon atom ratio and the oxygen to carbon atom ratio under different reaction conditions was observed by Van Krevelen (Figure 3d). In addition, the position labeling diagrams of several typical coals, cellulose, hemicellulose and lignin were compared [39]. It is also possible to see the trend in the coalification of Hydrochars. It can be seen that as the HTC temperature increases, the O/C and H/C of CS and SCS decrease towards the lower left. Hydrochar is close to the area of bituminous coal due to hydrolysis, dehydration, and decarboxylation, but the slope of SCS is more

pronounced. At 210–240 °C, the O/C and H/C of CS decrease by 0.08 (0.42–0.24) and 0.1 (1.29–1.19), respectively, and the O/C and H/C of SCS decrease by 0.13 (0.37–0.24) and 0.3 (1.27–0.97). It can be seen that the hydrolysis and small molecule condensation reaction of cellulose in SCS is better in this temperature range. SCS-HTC-270 had the lowest O/C and H/C of 0.17 and 0.82, respectively. It also shows that HTC can be prepared as more coal-like biomass fuel after acid washing.

The above proximate analysis and elemental analysis are related to HHV changes. As shown in Table S1 and Figure 3a, the HHV of CS was 16.3 MJ/kg and the HHV of CS-HTC-270 was 25.9 MJ/kg. With the increase of hydrothermal temperature, some low-energy chemical zones in CS will be transformed into high energy due to dehydration, decarboxylation, and other reactions, so that the HHV of hydrochars shows an upward trend. There are two main reasons for the increase of SCS calorific value: after acid washing pretreatment to remove ash, the combustible substances in the raw materials increased; and the C content increases. The HHV of the hydrochars of SCS is also higher than that of CS hydrochars, especially when the HTC temperature was increased to the range of 210–270 °C, because the content of cellulose increases, the HTC reaction becomes more complete, a large amount of volatiles in this temperature range is converted to a fixed carbon component, which is positive for HHV elevation [40]. The HHV has increased, even more, the HHV of SCS-HTC-270 could reach 27.7 MJ/kg.

It can be seen from Figure 3c and Table S1, The energy density trend is consistent with the HHV trend, with the energy density of SCS hydrochar increasing with HHV. Energy recovery efficiency (ERE) is an important parameter for evaluating the impact of HTC on solid fuel production. ERE is generally influenced by solid yield and energy density. The maximum value of ERE represents the optimum reaction conditions for the production of solid fuels. The ERE of SCS was highest at 210 °C, reaching 77.1%, decreasing to 60.8% at 270 °C. The decrease in the solid yield of hydrochars was the main reason for the decrease in ERE. The ERE of hydrochars from SCS was significantly higher than that of hydrochars from CS. The ERE of hydrochars from SCS reached 87.3% at 210 °C, which was 10.2% higher than that of hydrochars from CS. The improvement in efficiency is even greater at 240 °C, reaching 14%. This shows that the HTC of SCS has a better effect in the preparation of solid fuels. 180 °C is the most suitable temperature for the preparation of fuel by hydrothermal carbonization of SCS, which can reach 88.2%.

### 3.3. Structural Changes

#### 3.3.1. Analysis of the XRD

Based on the XRD analysis (Figure S1), when the CS values were approximately 15.5°, 22.7°, and 34.6° (representing the crystalline cellulose structure), three broad peaks were evident, which showed the coexistence of the amorphous state (hemicellulose, extract, lignin, and amorphous cellulose) and crystalline (crystalline cellulose) structures. After acid washing, some of the diffraction peaks became sharper, representing amorphous materials such as lignin and hemicellulose, while the degradation of crystalline cellulose increased. As the temperature of the HTC reaction increased, the crystal diffraction peaks of cellulose gradually disappeared and the peaks at 15.5° and 22.7° became wider. This indicates that high temperatures led to the degradation of crystalline cellulose and the amorphous formation of carbonaceous structures, which also characterizes the formation of hydrochar aromatization. The XRD analysis also shows that some metal elements and organic and inorganic compounds existed in CS. As shown in Figure S1a, HTC-270 has a peak between 21.37° and 23.7°, which gradually increases, indicating the presence of inorganic metal oxides or inorganic salts as the main ash components in hydrochars. The disappearance of this peak in SCS-HTC-270 in Figure S1b also represents the reduction of ash content in hydrochars of SCS, which is consistent with the results of FTIR analysis and proximate analysis.

### 3.3.2. Analysis of the FTIR

Figure 4 shows the FTIR analysis of CS, SCS, and their resulting hydrochars (180 °C, 210 °C, 240 °C, 270 °C) and provides information about the surface functional groups and their evolution during HTC. The functional group information can be verified by the above element analysis.

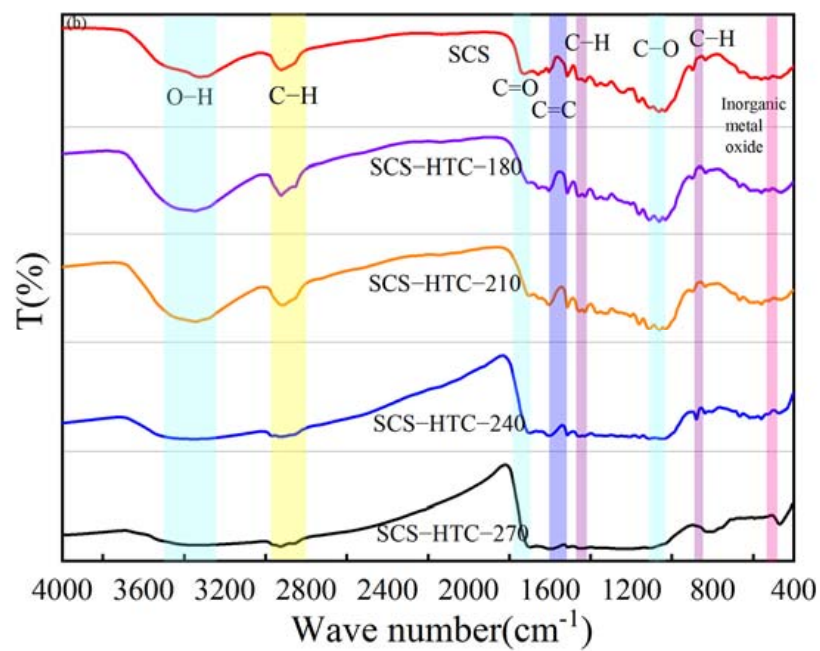
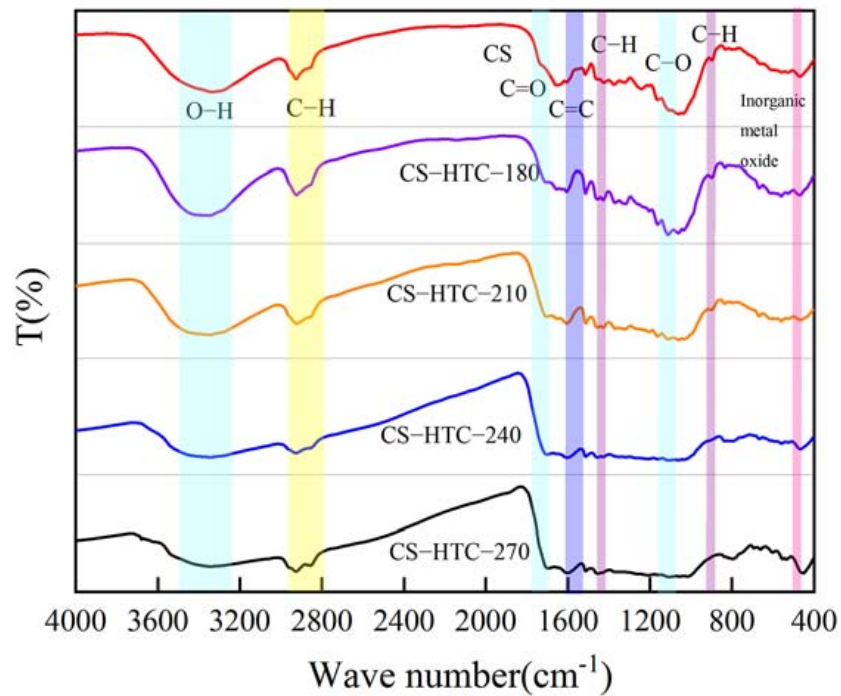


**Figure 4.** FTIR of CS, SCS and their hydrochar, (a) CS and (b) SCS.

Figure 4b shows the functional group information of the CS and hydrochars after acid washing. The main effect of acid washing on the CS is reflected in the two-part band:  $<600\text{ cm}^{-1}$  and  $>1400\text{ cm}^{-1}$ . The band  $<600\text{ cm}^{-1}$  belonged to inorganic metals and their oxides, which were reduced to varying degrees after acid washing [36,41]. The stretching vibrations of  $\text{CH}_3$ ,  $\text{CH}_2$ , and  $\text{CH}$  appeared near  $2922\text{ cm}^{-1}$ , indicating that CS methyl and methylene were released after acid washing. The changes of lignin at  $>1400\text{ cm}^{-1}$  were related to the change of lignin at  $1431\text{--}1450\text{ cm}^{-1}$ , which was related to the aromatic skeleton vibration and the in-plane deformation of C-H in the lignin [36,41]. The peak enhancement near  $1550\text{ cm}^{-1}$  may be due to the production of phenolic compounds. Near  $1733\text{ cm}^{-1}$  represents the disappearance of the C=O tensile vibration in the hemicellulose, indicating the hydrolysis of part of the hemicellulose [42]. The formation of soluble lignin and the hydrolysis of hemicellulose can be demonstrated.

As the HTC temperature increased,  $3200\text{--}3700\text{ cm}^{-1}$  represents that the water-containing O-H vibration will gradually decrease. In this part, the performance of SCS is more obvious than that of CS. This may be because the surface structure of the straw was destroyed after acid washing, resulting in increased hydrophobicity. The degree of dehydration during the carbonization process was strong, and the high hydrophobicity was important for fuel storage and handling because it provided high moisture resistance.  $1060\text{ cm}^{-1}$  and  $1160\text{ cm}^{-1}$  represent the C-O and C-O-C of cellulose [43]. The vibration of these two peaks disappears at  $210\text{ }^\circ\text{C}$ , which means that most of the cellulose in CS has been completely hydrolyzed. It disappears completely at  $240\text{ }^\circ\text{C}$  in SCS, indicating that after acid washing [41]. The chemical reaction of some components needs to be transferred to a higher temperature. Compared with the SCS-HTC-240, the change was obvious. The C=C and C-H stretching vibrations of the aromatic structure of SCS near  $1500\text{ cm}^{-1}$  and  $875\text{ cm}^{-1}$  are strengthened. It can be explained that the aromatization is strengthened by SCS's hydrochars at  $240\text{ }^\circ\text{C}$ , and  $2900\text{ cm}^{-1}$  represents aliphatic hydrocarbons and cycloalkanes. The gradual reduction of C-H (methylene and methyl) indicates that the dehydrogenation and deoxygenation reactions of SCS were greater.

### 3.4. Combustion Characteristics

CS, SCS, and its hydrochars are burned in a TG-DTG analyzer in a compressed air environment at a combustion temperature of  $50\text{--}900\text{ }^\circ\text{C}$ . The TG and DTG curves for different reaction conditions are shown in Figure 5. The combustion of the feedstock and hydrochars was divided into two stages. Therefore, to better evaluate the combustion characteristics of the fuel, it was divided into two successive stages based on two weight loss peaks. The first volatile phase burns in the range of  $260\text{--}340\text{ }^\circ\text{C}$  and the second in the range of  $350\text{--}450\text{ }^\circ\text{C}$  and is a fixed carbon combustion phase. Details of the combustion parameters are shown in Table 2, where both HTC and HTC after acid washing influence the combustion behavior of CS.

The ignition temperature ( $T_i$ ) and burn-out temperature ( $T_f$ ) of the hydrochars increased as the HTC temperature increased, from  $256\text{ }^\circ\text{C}$  and  $516\text{ }^\circ\text{C}$  for CS to  $314\text{ }^\circ\text{C}$  and  $541\text{ }^\circ\text{C}$  for CS-HTC-210. The increase in  $T_i$  content was mainly due to the degradation of hemicellulose and cellulose. The increase in  $T_f$  is mainly due to the degradation of hemicellulose and cellulose. The increase in the surface void structure and specific surface area of the biomass allows for better contact between oxygen and organic matter. As the temperature increases, the volatile content decreases and the voids are blocked by solid carbon; therefore, ignition is difficult. Therefore, the highest ignition rates are achieved at low volatile contents (e.g., CS-HTC-270). As the ash content in the hydrochars from SCS decreases, its volatile and fixed carbon content increases. The acid-washed HTC further prolongs the combustion process of the CS.

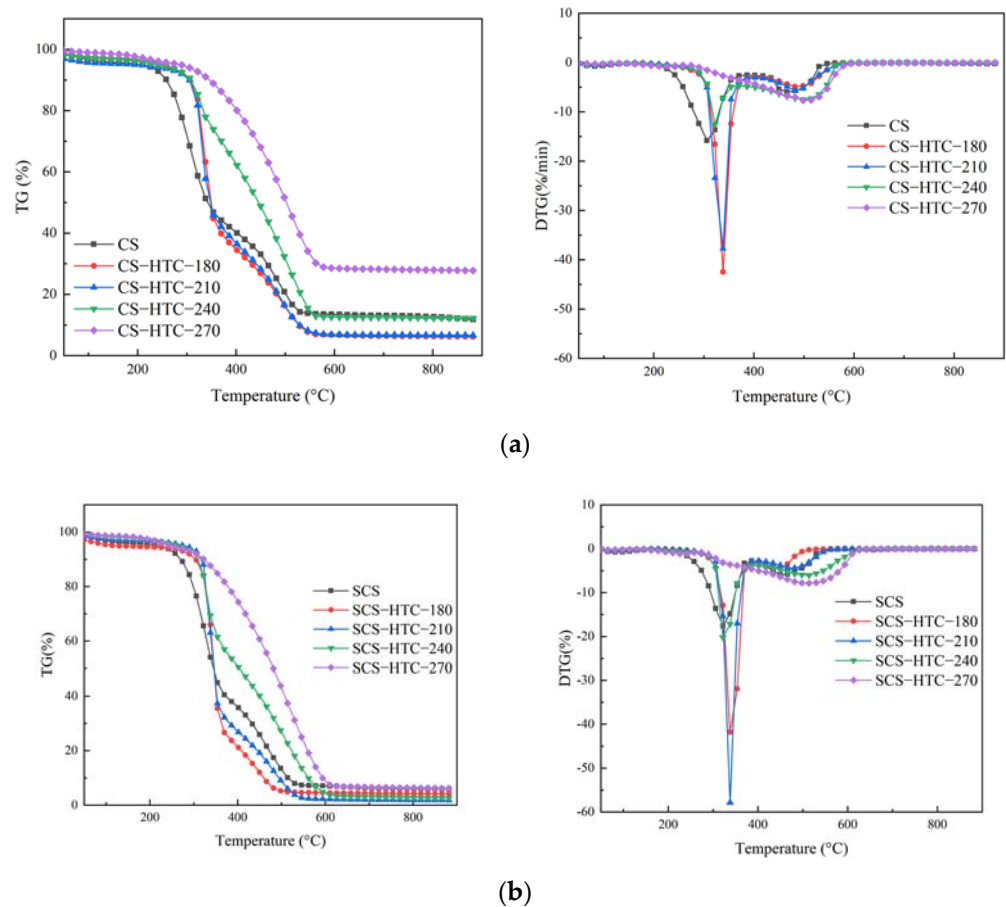


Figure 5. TG-DTG of CS, SCS, and their hydrochar, (a) CS and (b) SCS.

Table 2. Combustion characteristics parameters of CS, SCS, and their hydrochar.

Sample	Ti <sup>a</sup>	Tf <sup>b</sup>	Mfc <sup>c</sup>	T1 <sup>d</sup>	DTG1 <sup>e</sup>	T2 <sup>d</sup>	DTG2 <sup>e</sup>	DTGmean <sup>f</sup>	S	Rw
	(°C)	(°C)	(%/min)	(°C)	(%/min)	(°C)	(%/min)	(%/min)		
CS	257	517	16.3	311	−16.5	455	−6.8	−2.2	10.2	−12.3
CS-HTC180	313	538	8.5	338	−42.4	484	−4.8	−2.4	19.5	−25.1
CS-HTC210	318	541	8.3	334	−42.9	486	−5.7	−2.4	19.3	−25.3
CS-HTC240	325	550	14.5	324	−12.9	504	−7.5	−2.1	4.6	−7.2
CS-HTC270	366	558	30.2	-	-	508	−7.7	−1.7	1.72	−3.7
SCS	275	519	9.1	324	−17.7	452	−5.9	−2.4	10.4	−12.6
SCSHTC180	322	484	6.1	346	−53.1	450	−4.4	−2.5	26.2	−34.2
SCSHTC210	332	532	3.6	338	−57.8	476	−4.4	−2.6	25.8	−32.1
SCSHTC240	316	600	4.3	328	−24.2	508	−6	−2.4	10.4	−13.4
SCSHTC270	344	600	8.7	326	−3.3	512	−7.9	−2.2	2.46	3.76

<sup>a</sup> Ti the Ignition temperature. <sup>b</sup> Tf the burnout temperature. <sup>c</sup> Mf the residual mass. <sup>d</sup> T1, T2, the temperature according to the first loss peak, and the second loss peak. <sup>e</sup> DTG1, DTG2, the weight loss rate according to the first loss peak, the second loss peak. <sup>f</sup> DTGmean the average weight loss rate.

The comprehensive combustion index (S) and combustion stability index (Rw) are the key to evaluating fuel combustion performance [13]. As can be seen from Table 2, both acid washing and HTC will improve the S index. For S value, weight loss at the first stage, namely volatile combustion, is the key influencing factor. Volatiles can improve flame combustion and reactivity. After acid washing, due to the removal of ash, the volatile content is increased, and the combustion stability of hemicellulose with the worst thermal stability can be further improved. Therefore, the S value and Rw value of SCS can reach 10.4 ( $10^{-7} \times \text{min}^{-2} \times \text{°C}^{-3}$ ) and  $-12.6 (10^{-5} \times \text{min}^{-1} \times \text{°C}^{-2})$ . The influence of HTC on S value is positive. The S value and Rw of CS-HTC-180 can reach 19.5 ( $10^{-7} \times \text{min}^{-2} \times \text{°C}^{-3}$ ) and  $-25.3 (10^{-5} \times \text{min}^{-1} \times \text{°C}^{-2})$ . However, with dehydration and decarboxylation in hydrothermal carbonization, the decrease of volatiles also represents the decrease of S

and  $R_w$  values. After acid washing, the hydrolysis degree of cellulose in hydrothermal carbonization increased, the ash content decreased, and the release degree of volatile compounds increased. The best  $S$  and  $R_w$  values are  $26.0 (10^{-7} \times \text{min}^{-2} \times \text{°C}^{-3})$  and  $-34.2 (10^{-5} \times \text{min}^{-1} \times \text{°C}^{-2})$  of SCS-HTC-180.

#### 4. Conclusions

In conclusion, due to a large amount of AAEM removal and the change of biomass composition, the HTC after acid washing pretreatment which reduces ash content is beneficial to improve the HTC effect. Compared with the hydrochars without acid washing pretreatment, the hydrochars prepared by HTC after acid washing has higher HHV (27.7 MJ/kg), deeper coalification degree, and higher energy recovery efficiency with the increase of energy density (87.31%). The increase of volatiles and fixed carbon content in the hydrochars generated after acid washing also makes the combustion characteristics of the hydrochars better, and the optimal condition is the hydrothermal carbonized carbon generated after acid washing at 180 °C. Therefore, HTC after acid washing pretreatment can be a new method for converting biomass waste to produce renewable energy.

**Supplementary Materials:** The following supporting information can be downloaded at: <https://www.mdpi.com/article/10.3390/en15051828/s1>, Figure S1: XRD analysis of CS, SCS and their hydrochar; Table S1: Fuel properties of hydrochars.

**Author Contributions:** Conceptualization, M.C. and X.X.; methodology, S.H. and L.B.; validation, L.B. and M.C.; investigation, S.H., Z.C. and K.Y.; data curation, S.H. and M.C.; writing—original draft preparation, S.H.; writing—review and editing, L.B.; funding acquisition, L.B. and M.C. All authors have read and agreed to the published version of the manuscript.

**Funding:** This work was supported by the National Natural Science Foundation of China (52070088), National Natural Science Foundation of China (52100146), and Jilin Science and Technology Bureau Outstanding Young Talents Training Special Project (No. 20200104118). Scientific Research Project of Education Department of Jilin Province (No. JJKH20210263KJ). The Ministry of housing and urban-rural development of china(2021-K-118).The research collaboration among the groups and universities of the authors is also grateful.

**Institutional Review Board Statement:** Not applicable.

**Informed Consent Statement:** Not applicable.

**Data Availability Statement:** Data is contained within the article.

**Conflicts of Interest:** The authors declare no conflict of interest.

#### References

1. Wei, J.; Liang, G.; Alex, J.; Zhang, T.; Ma, C. Research Progress of Energy Utilization of Agricultural Waste in China: Bibliometric Analysis by Citespace. *Sustainability* **2020**, *12*, 812. [CrossRef]
2. Zhang, L.; Xu, C.C.; Champagne, P. Overview of recent advances in thermo-chemical conversion of biomass. *Energy Convers. Manag.* **2010**, *51*, 969–982. [CrossRef]
3. Goldemberg, J.; Coelho, S. Renewable energy—Traditional biomass vs. modern biomass. *Energy Policy* **2004**, *32*, 711–714. [CrossRef]
4. Wang, L.; Jin, X.; Wang, Q.; Mao, H.; Liu, Q.; Weng, G.; Wang, Y. Spatial and temporal variability of open biomass burning in Northeast China from 2003 to 2017. *Atmos. Ocean. Sci. Lett.* **2020**, *13*, 240–247. [CrossRef]
5. Wang, R.; Lei, H.; Liu, S.; Ye, X.; Jia, J.; Zhao, Z. The redistribution and migration mechanism of nitrogen in the hydrothermal co-carbonization process of sewage sludge and lignocellulosic wastes. *Sci. Total Environ.* **2021**, *776*, 145922. [CrossRef]
6. Pauline, A.L.; Joseph, K. Hydrothermal carbonization of organic wastes to carbonaceous solid fuel—A review of mechanisms and process parameters. *Fuel* **2020**, *279*, 118472. [CrossRef]
7. Yan, W.; Perez, S.; Sheng, K. Upgrading fuel quality of moso bamboo via low temperature thermochemical treatments: Dry torrefaction and hydrothermal carbonization. *Fuel* **2017**, *196*, 473–480. [CrossRef]
8. Lucian, M.; Volpe, M.; Merzari, F.; Wüst, D.; Kruse, A.; Andreottola, G.; Fiori, L. Hydrothermal Carbonization coupled with Anaerobic Digestion for the valorization of the Organic Fraction of Municipal Solid Waste. *Bioresour. Technol.* **2020**, *314*, 123734. [CrossRef]

9. Román, S.; Ledesma, B.; Álvarez, A.; Coronella, C.; Qaramaleki, S. Suitability of hydrothermal carbonization to convert water hyacinth to added-value products. *Renew. Energy* **2020**, *146*, 1649–1658. [[CrossRef](#)]
10. Kambo, H.S.; Dutta, A. A comparative review of biochar and hydrochar in terms of production, physico-chemical properties and applications. *Renew. Sustain. Energy Rev.* **2015**, *45*, 359–378. [[CrossRef](#)]
11. Wilk, M.; Magdziarz, A.; Kalemba-Rec, I.; Szymańska-Chargot, M. Upgrading of green waste into carbon-rich solid biofuel by hydrothermal carbonization: The effect of process parameters on hydrochar derived from acacia. *Energy* **2020**, *202*, 117717. [[CrossRef](#)]
12. Pawlak-Kruczek, H.; Niedzwiecki, L.; Sieradzka, M.; Mlonka-Mędrala, A.; Baranowski, M.; Serafin-Tkaczuk, M.; Magdziarz, A. Hydrothermal carbonization of agricultural and municipal solid waste digestates—Structure and energetic properties of the solid products. *Fuel* **2020**, *275*, 117837. [[CrossRef](#)]
13. Zhang, C.; Ma, X.; Chen, X.; Tian, Y.; Zhou, Y.; Lu, X.; Huang, T. Conversion of water hyacinth to value-added fuel via hydrothermal carbonization. *Energy* **2020**, *197*, 117193. [[CrossRef](#)]
14. Román, S.; Nabais, J.M.V.; Laginhas, C.; Ledesma, B.; González, J.F.G. Hydrothermal carbonization as an effective way of densifying the energy content of biomass. *Fuel Process. Technol.* **2012**, *103*, 78–83. [[CrossRef](#)]
15. Park, K.Y.; Lee, K.; Kim, D. Characterized hydrochar of algal biomass for producing solid fuel through hydrothermal carbonization. *Bioresour. Technol.* **2018**, *258*, 119–124. [[CrossRef](#)]
16. Cai, J.; Li, B.; Chen, C.; Wang, J.; Zhao, M.; Zhang, K. Hydrothermal carbonization of tobacco stalk for fuel application. *Bioresour. Technol.* **2016**, *220*, 305–311. [[CrossRef](#)]
17. Lu, X.; Pellechia, P.J.; Flora, J.R.; Berge, N.D. Influence of reaction time and temperature on product formation and characteristics associated with the hydrothermal carbonization of cellulose. *Bioresour. Technol.* **2013**, *138*, 180–190. [[CrossRef](#)]
18. Yan, M.; Weng, Z.; Prabowo, B.; Setyobudi, R.H.; Birowosuto, M.D. Efficient production of high calorific value solid fuel from palm oil empty fruit bunch by pressurized hydrothermal carbonization. *Sustain. Energy Technol. Assess.* **2019**, *34*, 56–61.
19. Reza, M.T.; Rottler, E.; Herklotz, L.; Wirth, B. Hydrothermal carbonization (HTC) of wheat straw: Influence of feedwater pH prepared by acetic acid and potassium hydroxide. *Bioresour. Technol.* **2015**, *182*, 336–344. [[CrossRef](#)]
20. Yao, C.; Shin, Y.; Wang, L.-Q.; Windisch, C.F.; Samuels, W.D.; Arey, B.W.; Wang, C.; Risen, W.M.; Exarhos, G.J. Hydrothermal Dehydration of Aqueous Fructose Solutions in a Closed System. *J. Phys. Chem. C* **2007**, *111*, 15141–15145. [[CrossRef](#)]
21. Keiluweit, M.; Nico, P.S.; Johnson, M.G.; Kleber, M. Dynamic Molecular Structure of Plant Biomass-Derived Black Carbon (Biochar). *Environ. Sci. Technol.* **2010**, *44*, 1247–1253. [[CrossRef](#)] [[PubMed](#)]
22. Fang, Z.; Sato, T.; Smith, R.L.; Inomata, H.; Arai, K.; Kozinski, J.A. Reaction chemistry and phase behavior of lignin in high-temperature and supercritical water. *Bioresour. Technol.* **2008**, *99*, 3424–3430. [[CrossRef](#)] [[PubMed](#)]
23. Reza, M.T.; Lynam, J.; Uddin, M.H.; Coronella, C.J. Hydrothermal carbonization: Fate of inorganics. *Biomass-Bioenergy* **2013**, *49*, 86–94. [[CrossRef](#)]
24. Funke, A.; Ziegler, F. Hydrothermal carbonization of biomass: A summary and discussion of chemical mechanisms for process engineering. *Biofuels Bioprod. Biorefining* **2010**, *4*, 160–177. [[CrossRef](#)]
25. Lane, D.J.; van Eyk, P.J.; Ashman, P.J.; Kwong, C.W.; de Nys, R.; Roberts, D.A.; Cole, A.J.; Lewis, D.M. Release of Cl, S, P, K, and Na during Thermal Conversion of Algal Biomass. *Energy Fuels* **2015**, *29*, 2542–2554. [[CrossRef](#)]
26. de Carvalho, D.M.; Sevastyanova, O.; Penna, L.S.; da Silva, B.P.; Lindström, M.E.; Colodette, J.L. Assessment of chemical transformations in eucalyptus, sugarcane bagasse and straw during hydrothermal, dilute acid, and alkaline pretreatments. *Ind. Crops Prod.* **2015**, *73*, 118–126. [[CrossRef](#)]
27. Yang, J.; Feng, Z.; Gao, Q.; Ni, L.; Hou, Y.; He, Y.; Liu, Z. Ash thermochemical behaviors of bamboo lignin from kraft pulping: Influence of washing process. *Renew. Energy* **2021**, *174*, 178–187. [[CrossRef](#)]
28. Cao, S.; Pu, Y.; Studer, M.; Wyman, C.; Ragauskas, A.J. Chemical transformations of *Populus trichocarpa* during dilute acid pretreatment. *RSC Adv.* **2012**, *2*, 10925–10936. [[CrossRef](#)]
29. Roy, R.; Rahman, S.; Raynie, D.E. Recent advances of greener pretreatment technologies of lignocellulose. *Curr. Res. Green Sustain. Chem.* **2020**, *3*, 100035. [[CrossRef](#)]
30. Yao, Z.; Ma, X. Hydrothermal carbonization of Chinese fan palm. *Bioresour. Technol.* **2019**, *282*, 28–36. [[CrossRef](#)]
31. Sluiter, A.; Hames, B.; Ruiz, R.; Scarlata, C.; Sluiter, J.; Templeton, D.; Crocker, D.L.A.P. *Determination of Structural Carbohydrates and Lignin in Biomass*; Technical Report NREL/TP-510-42618; National Renewable Energy Laboratory: Golden, CO, USA, 2010.
32. Parshetti, G.; Hoekman, S.K.; Balasubramanian, R. Chemical, structural and combustion characteristics of carbonaceous products obtained by hydrothermal carbonization of palm empty fruit bunches. *Bioresour. Technol.* **2013**, *135*, 683–689. [[CrossRef](#)] [[PubMed](#)]
33. Huang, N.; Zhao, P.; Ghosh, S.; Feduykhin, A. Co-hydrothermal carbonization of polyvinyl chloride and moist biomass to remove chlorine and inorganics for clean fuel production. *Appl. Energy* **2019**, *240*, 882–892. [[CrossRef](#)]
34. Chaiwat, W.; Hasegawa, I.; Kori, J.; Mae, K. Examination of Degree of Cross-Linking for Cellulose Precursors Pretreated with Acid/Hot Water at Low Temperature. *Ind. Eng. Chem. Res.* **2008**, *47*, 5948–5956. [[CrossRef](#)]
35. Mourant, D.; Wang, Z.; He, M.; Wang, X.S.; Garcia-Perez, M.; Ling, K.; Li, C.Z. Mallee wood fast pyrolysis: Effects of alkali and alkaline earth metallic species on the yield and composition of bio-oil. *Fuel* **2011**, *90*, 2915–2922. [[CrossRef](#)]
36. Chen, D.; Gao, D.; Capareda, S.C.; Huang, S.; Wang, Y. Effects of hydrochloric acid washing on the microstructure and pyrolysis bio-oil components of sweet sorghum bagasse. *Bioresour. Technol.* **2019**, *277*, 37–45. [[CrossRef](#)]

37. Chen, X.; Ma, X.; Peng, X.; Lin, Y.; Yao, Z. Conversion of sweet potato waste to solid fuel via hydrothermal carbonization. *Bioresour. Technol.* **2018**, *249*, 900–907. [[CrossRef](#)]
38. Bobleter, O. Hydrothermal degradation of polymers derived from plants. *Prog. Polym. Sci.* **1994**, *19*, 797–841. [[CrossRef](#)]
39. Kim, D.; Lee, K.; Park, K.Y. Upgrading the characteristics of biochar from cellulose, lignin, and xylan for solid biofuel production from biomass by hydrothermal carbonization. *J. Ind. Eng. Chem.* **2016**, *42*, 95–100. [[CrossRef](#)]
40. El-Sayed, S.A.; Mostafa, M.E. Kinetic Parameters Determination of Biomass Pyrolysis Fuels Using TGA and DTA Techniques. *Waste Biomass-Valorization* **2015**, *6*, 401–415. [[CrossRef](#)]
41. Chen, D.; Gao, D.; Capareda, S.C.; Shuang, E.; Jia, F.; Wang, Y. Influences of hydrochloric acid washing on the thermal decomposition behavior and thermodynamic parameters of sweet sorghum stalk. *Renew. Energy* **2020**, *148*, 1244–1255. [[CrossRef](#)]
42. Ma, Q.; Han, L.; Huang, G. Effect of water-washing of wheat straw and hydrothermal temperature on its hydrochar evolution and combustion properties. *Bioresour. Technol.* **2018**, *269*, 96–103. [[CrossRef](#)] [[PubMed](#)]
43. Guo, S.; Dong, X.; Wu, T.; Shi, F.; Zhu, C. Characteristic evolution of hydrochar from hydrothermal carbonization of corn stalk. *J. Anal. Appl. Pyrolysis* **2015**, *116*, 1–9. [[CrossRef](#)]